

Higher order spacing ratios in random matrix theory and complex quantum systems

S. Harshini Tekur,^{1,*} Udaysinh T. Bhosale,^{1,†} and M. S. Santhanam^{1,‡}

¹Indian Institute of Science Education and Research, Dr. Homi Bhabha Road, Pune 411 008, India

The distribution of the ratios of nearest neighbor level spacings has become a popular indicator of spectral fluctuations in complex quantum systems like interacting many-body localized and thermalization phases, quantum chaotic systems, and also in atomic and nuclear physics. In contrast to the level spacing distribution, which requires the cumbersome and at times ambiguous unfolding procedure, the ratios of spacings do not require unfolding and are easier to compute. In this work, for the class of Wigner-Dyson random matrices with nearest neighbor spacing ratios r distributed as $P_\beta(r)$ for the three ensembles indexed by $\beta = 1, 2, 4$, their k -th order spacing ratio distributions are shown to be identical to $P_{\beta'}(r)$, where β' , an integer, is a function of β and k . This result is shown for Gaussian and circular ensembles of random matrix theory and for several physical systems such as spin chains, chaotic billiards, Floquet systems and measured nuclear resonances.

Spectral fluctuations in complex quantum systems contain information about their physical character. In tight binding models and crystalline lattices that display metal to insulator transition, the metallic and insulator regimes are distinguishable based on their spectral fluctuations¹. In interacting spin chains, many body localized and thermal phases also carry distinct spectral signatures². In quantum systems with chaotic classical limit³, the fluctuations indicate if the system is integrable, chaotic or a mixture of both these types of dynamics⁴.

Of the spectral fluctuation measures modeled through random matrix theory (RMT), the most popular one is the nearest neighbor level spacings, $s_i = E_{i+1} - E_i$, where $E_i, i = 1, 2, \dots$ are the discrete eigenvalues of a quantum operator. For time-reversal invariant systems without spin degree of freedom, RMT predicts that the spacings are Wigner distributed⁵, $P(s) = (\pi/2)s \exp(-\pi s^2/4)$ indicating the presence of level repulsion. In physical systems, Wigner distribution is associated with the metallic regime of tight binding models⁶, thermal phase of many-body systems⁷, chaotic quantum systems⁸ such as coupled oscillators⁹ and atoms in strong external fields¹⁰ and many others¹¹. This is in contrast to the class of integrable systems which display level clustering through Poissonian spacing distribution, $P(s) = \exp(-s)$.

In practice, spacing distributions have to be computed after removing the system dependent spectral features, i.e, the average part of the density of states, through a cumbersome and non-unique numerical procedure of unfolding the spectra. Further, in many-body systems (for example, Bose-Hubbard model) at large interaction strengths, the density of states is not a smooth function of energy and hence separating it into an average and fluctuating part, a pre-requisite for spectral unfolding, becomes non-trivial^{13,14}.

These difficulties have been overcome through the use of spacing ratio¹³ $r_i = s_{i+1}/s_i, i = 1, 2, \dots$, since it does not depend on the local density of states and consequently does not require unfolding. The RMT averages for the spacing ratios, drawn from three standard random matrix ensembles with co-dimension $\beta = 1, 2$ and 4 corresponding to the Gaussian orthogonal ensemble

(GOE), unitary ensemble (GUE) and symplectic ensemble (GSE), have been obtained as^{15,16},

$$P(r, \beta) = C_\beta \frac{(r + r^2)^\beta}{(1 + r + r^2)^{1 + \frac{3}{2}\beta}}, \quad (1)$$

where C_β is a constant that depends on β .

However, few results exist for the distribution of non-overlapping higher order spacing ratio¹⁷ defined by

$$r_i^{(k)} = \frac{s_{i+k}^{(k)}}{s_i^{(k)}} = \frac{E_{i+2k} - E_{i+k}}{E_{i+k} - E_i}, \quad i, k = 1, 2, 3, \dots \quad (2)$$

Nearest neighbor spacing ratio r probes fluctuations in spectral scales of the order of unit mean spacing, whereas $r^{(k)}$ probes fluctuations in spectral interval of k mean spacings. In many physical situations, knowledge of spectral fluctuations at larger spectral intervals is useful. For quantum chaotic systems with a classical limit, semiclassical theories¹⁸ dictate that the higher order spectral fluctuations would be related to short time periodic orbits, effectively acting as a probe of short time dynamics⁸, at times shorter than Heisenberg time scale. The rare-region effects or Griffith effects¹⁹ in the vicinity of many-body localization transition influences the transport and entanglement properties whose time-scales can be probed by the higher order spacing ratios.

Thus, higher order spacing ratios have profound physical implications apart from being an intrinsic object of interest in random matrix theory. In this work, for the random matrices, of order $N \gg 1$, belonging to the Gaussian and circular ensemble of random matrix theory, we present compelling numerical evidence to demonstrate an elegant relation between non-overlapping k -th order spacing ratio distribution $P^k(r, \beta)$ and the nearest neighbor spacing ratio distribution $P(r, \beta')$:

$$P^k(r, \beta) = P(r, \beta'), \quad \beta = 1, 2, 4, \quad (3)$$

$$\beta' = \frac{k(k+1)}{2}\beta + (k-1), \quad k \geq 1. \quad (4)$$

This scaling relation is the central result of this paper. Note that $4 \leq \beta' < \infty$ can take large integer values and,

unlike $\beta = 1, 2, 4$, does not have corresponding random matrix model as yet. Thus, Eq. 3 may be considered as a generalization of the Wigner surmise. It is also pertinent to point out that similar relation between the higher order and nearest neighbor *spacing distributions* had been proposed earlier without rigorous proof^{21,22}, though their validity had never been tested on spectra from random matrices or physical systems. One exception is the well-known relation that the next-nearest neighbor ($k = 2$) level spacings of levels from circular orthogonal ensemble are distributed as the nearest neighbor ($k = 1$) spacings of levels from circular symplectic ensemble²³. In the limit of large matrix dimensions, this is known to hold good for the corresponding Gaussian ensemble as well.

Remarkably, the functional form of $P^k(r, \beta)$ is identical to $P(r, \beta')$ with order of the spacing ratio k and Dyson index β dependence entering through the modified parameter β' . In the rest of the paper, numerical evidence from random matrices and from physical systems such as spin chain, quantum billiards and measured nuclear resonances are presented, apart from some well-studied models of quantum chaos like the kicked top and the intermediate map. Further, Eq. 3 suffers from strong finite size effects and we discuss disparate cases that have different rates of convergence to Eq. 4.

Random matrix spectra : First, Eqs. 3-4 are verified for the spectra drawn from random matrix ensembles. The eigenvalues of random matrices (drawn from Gaussian ensembles) of order $N = 10^5$ are computed for $\beta = 1, 2$ and 4. The resulting histograms of higher order spacing ratios shown in Fig. 1 are averaged over 1000 realizations. It is compared against $k = 1$ spacing ratio distribution with β' as given in Eq. 1. The solid curves in this figure represents $P(r, \beta')$ and its excellent agreement with the histograms points to the validity of Eq. 3. As the inset in these figures reveal, the best match of $P(r, \beta')$ with the histograms is obtained precisely for the value of β' predicted by Eq. 4. The scaling in Eqs. 3-4 holds good for the circular ensembles of random matrix theory as well. An excellent agreement with the postulated scaling relation is seen for the circular orthogonal, unitary and symplectic ensembles (COE, CUE, and CSE respectively) as well, and is not shown here as the corresponding distributions are identical to those in Fig. 1.

Further, to quantitatively check that that value of β' predicted by Eq. 4 is the one that best fits the histogram $P^k(r, \beta)$ obtained from random matrix simulations, we compute the difference between the cumulative distributions defined as,

$$D(\beta') = \sum_i |I^k(r, \beta) - I(r_i, \beta')|, \quad (5)$$

where $I(r, \beta')$ and $I^k(r, \beta)$ are the cumulative distributions corresponding, respectively, to $P(r, \beta')$ and $P^k(r, \beta)$. Then, the value of β' for which $D(\beta')$ is minimum is the one that best fits the observed histogram, and this remarkably coincides with the value predicted by Eq. 4. The insets in Fig. 1 display the quantitative verifica-

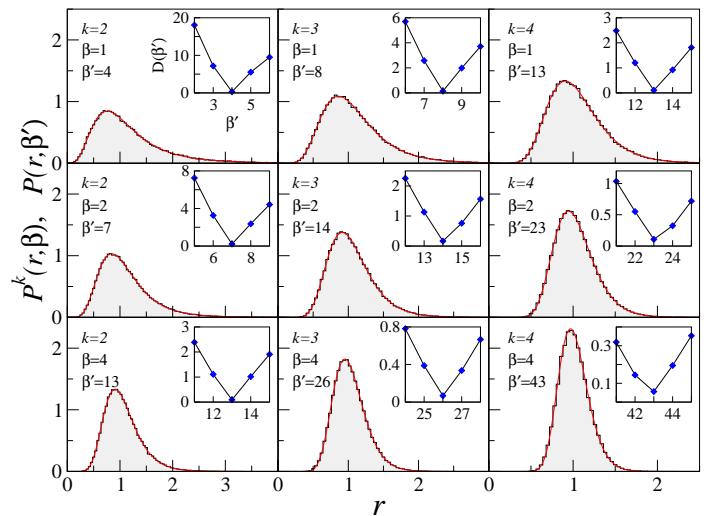


FIG. 1. Distribution of higher order spacing ratios (histograms) for the spectra of random matrices drawn from GOE, GUE and GSE and the distribution $P(r, \beta')$ (solid line) with β' given by Eq. 4. (Inset) shows D as a function of β' .

tion of scaling in Eqs. 3-4. As an additional verification, the Kolmogorov-Smirnov test²⁴ has been performed for this data, and the p -values obtained indicate that the given data corresponds to the predicted distribution in Eq. 3 with a high probability.

Many-body systems (GOE class): Figure 2 shows validity of the scaling relation (Eqs. 3-4) for two many-body systems, namely, (i) a one-dimensional spin-1/2 chain with a defect located at its center²⁵, and (ii) for experimentally measured nuclear resonances of the Erbium atom²⁶. Both are examples of many-body systems whose nearest-neighbor spectral statistics has been well-established to coincide with that of GOE. The eigenvalues for the spin chain are obtained by diagonalizing the Hamiltonian

$$H = \sum_{i=1}^L \omega S_i^z + \epsilon_d S_d^z + \sum_{i=1}^{L-1} [J_{xy}(S_i^x S_{i+1}^x + S_i^y S_{i+1}^y) + J_z S_i^z S_{i+1}^z]. \quad (6)$$

Here, $S_i^{x,y,z}$ are the spin operators in three directions, acting on site i . The first term of the Hamiltonian represents a static magnetic field in the z -direction, accounting for a Zeeman splitting of strength ω at all sites, except the defect site d where it is $\epsilon_d + \omega$. The second term, by itself is the well-known XXZ Hamiltonian, and couples nearest-neighbor spins in all directions, with J_{xy} (taken here to be 1) being coupling strength along x - and y - directions, and J_z (taken as 0.5) that along the z -direction. For the spectra from the Hamiltonian in Eq. 6, the upper panel of Fig. 2 displays a good agreement between the computed k -th spacing ratio distribution and $P(r, \beta')$ given by Eqs. 3-4. Finite size effects have been discussed with

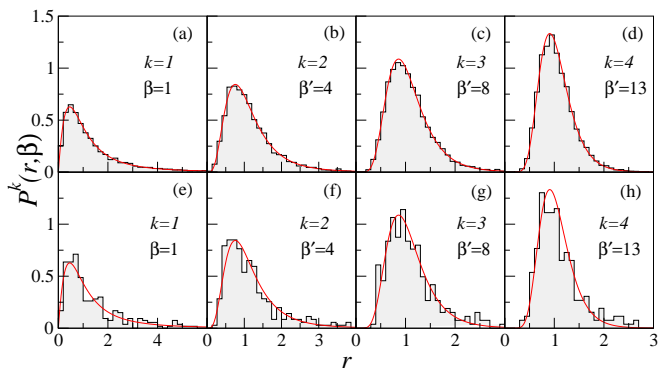


FIG. 2. (Color online) Distribution of k -th spacing ratio distribution two many-body systems of the GOE class ($\beta = 1$). The histograms correspond to the distributions obtained from the spectra from a disordered spin chain (upper panel) and nuclear resonance of ^{167}Er atom (lower panel). The solid line corresponds to $P(r, \beta')$ predicted by Eqs. 3-4, with $\beta' = 1, 4, 8$ and 13 for $k = 1$ to 4 .

respect to this system in Fig. 5(c), by considering different values for the length L of the chain, which changes the dimension of the Hilbert space to be diagonalized. For the distributions shown in Figs.2(a),(b),(c),(d), the length of the spin chain was considered to be $L = 14$, the site of the disorder was taken to be $L/2$, and the magnitude of the disorder was $\epsilon_d = 0.5$. A similar excellent agreement can be inferred from the lower panel of Fig.2 for the experimentally measured data for neutron resonances for the Erbium atom²⁶. Even with only about 200 measured resonances, a good agreement with the theoretical form of $P^k(r, \beta')$ is observed for $k = 1$ to 4 . For both these systems, the nearest neighbor spacing distribution was observed to follow the Wigner surmise, and we observe here that it holds for the ratio distributions as well, with $D(\beta')$ as determined for these, confirming the observation.

Disordered spin chain and quantum chaotic system (GUE class): Next, the validity of Eqs. 3-4 for two physical systems belonging to GUE symmetry class is discussed. They are, (i) a one-dimensional disordered spin-1/2 system²⁷, and (ii) a quantum billiard in a static magnetic field with one of its walls having an attached ferrite strip²⁸. Both these systems are not invariant under time reversal symmetry and hence belong to GUE class. The Hamiltonian for the disordered spin chain is

$$H = \sum_{i=1}^L [J_1(\mathbf{S}_i \cdot \mathbf{S}_{i+1}) + h_i S_i^z + J_2(\mathbf{S}_i \cdot (\mathbf{S}_{i+1} \times \mathbf{S}_{i+2}))], \quad (7)$$

in which J_1 and J_2 represent strength of coupling between sites. The first term (by itself, the Heisenberg spin chain) corresponds to nearest neighbor couplings in all directions, with J_1 giving the strength of the coupling. The second term introduces a Gaussian distributed, random magnetic field of mean 0 and strength h_i in the

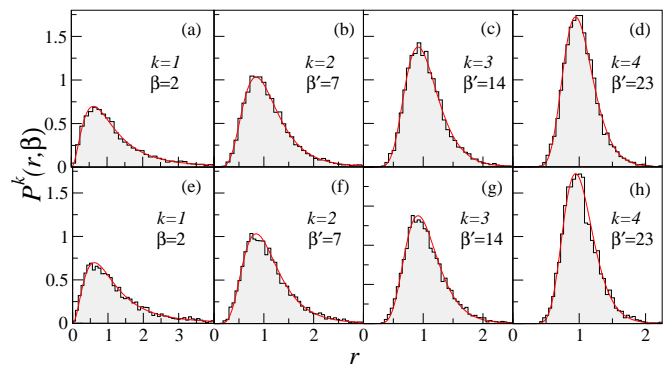


FIG. 3. (Color online) Distribution of k -th spacing ratio distribution two physical systems of the GUE class ($\beta = 2$), a spin chain with a three-spin interaction (upper panel), and chaotic billiards with a magnetized ferrite strip (lower panel). The solid line corresponds to the predicted $P(r, \beta')$, with $\beta' = 2, 7, 14$ and 23 for $k = 1$ to 4 .

z -direction. The third term breaks time reversal symmetry by introducing a three-spin interaction with the nearest as well as the next-nearest neighbor couplings with strength J_2 . The parameters used to obtain data for Figs. 3(a),(b),(c),(d) are $L = 12$, $h/J_1 = 1$ and $J_2/J_1 = 1$, with open boundary conditions. The computed spacing ratio distribution $P^k(r_i, \beta = 2)$ shown in the upper panel of Fig. 3 for $k = 2, 3, 4$ is well described by $P(r, \beta')$.

The quantum chaotic billiards²⁸ (of size ~ 17 inches) considered here consists of a rectangle with two adjacent walls replaced by circular arcs, and a third wall having a thin ferrite strip (of thickness ~ 0.09 inches) attached to it. On applying a static magnetic field, time reversal symmetry is broken and being a chaotic system its eigenvalue fluctuations coincide with GUE statistics. The eigenvalues were computed by solving the Helmholtz equation with suitable boundary conditions. As seen in lower panel of Fig. 3, the distribution of k -th spacing ratios provides another instance of the validity of the scaling relation in Eqs. 3-4 for GUE systems with $\beta = 2$ for GUE systems.

Spectra of Floquet systems: The validity of Eq. 3-4 has also been tested for time-dependent systems whose time-evolution operators (Floquet matrices) have unimodular eigenvalues. Their fluctuation properties are modeled by those of circular random matrix ensembles. One relevant model is the quantum kicked top whose classical limit is chaotic²⁹. As this system is periodically kicked, the quantum version can be studied in terms of the unitary time evolution operator

$$\hat{U} = \exp(-iqJ_z^2/2) \exp(-ipJ_y), \quad (8)$$

where $q = 10$ is the kick strength that acts as chaos parameter and $p = 1.7$. The action of this operator on a particle of angular momentum \mathbf{J} , taken to be 200 here, is a precession about the y -axis, followed by state-dependent rotation about the z -axis (as a consequence of periodic

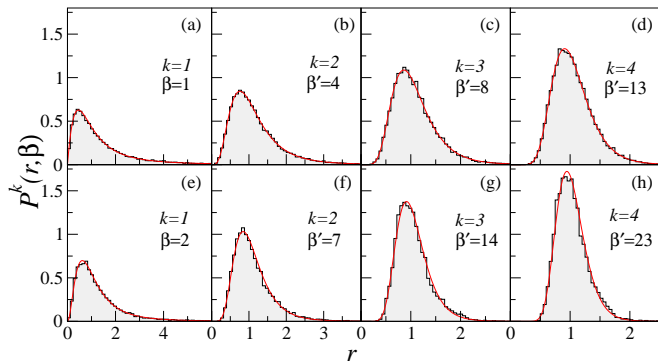


FIG. 4. (Color online) The distribution of the k -th spacing ratios, for $k=1, 2, 3, 4$ is shown two Floquet systems –the kicked top, belonging to the COE class (upper panel), and the intermediate map, belonging to the CUE class, (lower panel) respectively. The histograms are obtained from determining the k -th spacing ratios from the eigenvalues of the systems, and the solid line corresponds to $P(r, \beta')$, with $\beta' = 1, 4, 8, 13$ for COE and $\beta' = 2, 7, 14, 23$ for CUE.

kicking). The eigenvalues of \hat{U} are computed by diagonalizing this operator and its fluctuations are well-known to be consistent with COE statistics²⁹. Figure 4 (upper panel) shows the k -th spacing ratio distribution for this system which, as anticipated from Eqs. 3-4, follows $P(r, \beta')$ with $\beta'=1$, following COE statistics.

As another instance of CUE class ($\beta = 2$), a unitary operator corresponding to the so-called intermediate map is considered. The quantum version of this map has been investigated previously in the context of multifractal eigenstates, and in a specified range, has spectral fluctuations similar to CUE matrices³⁰. The unitary operator can be written in terms of an $N \times N$ matrix as

$$U_{ab} = \frac{\exp(-i\phi_a)}{N} \frac{1 - \exp[i2\pi\gamma N]}{1 - \exp[i2\pi(a - b + \gamma N)/N]}, \quad (9)$$

with $N(= 12000)$ being the dimension of the Hilbert space. Here, ϕ_a is a random variable uniformly distributed between $[0, 2\pi]$, and for any irrational γ , the spectral statistics are of the CUE type. The distribution of k -th spacing ratios for this system is shown in Fig. 4 (lower panel) and is seen to be in agreement with Eqs. 3-4.

The scaling relation in Eqs. 3-4 suffers from finite size effects to the extent that different systems converge to the scaling relation at different rates, especially if $k \gg 1$. In the spectra of physical systems as well as in the random matrices of the Gaussian and Circular ensembles, it was observed in practice that for higher order spacing ratios, say $k > 5$, the value of β' obtained by fitting $P(r, \beta')$ to the empirical distribution did not quite agree with that predicted by Eq. 4. It is seen that the convergence to the predicted β' is strongly pronounced as the order N of the random matrix increases. This is illustrated in Fig 5 for two distinct values of k . In one case, for $k = 9$ and

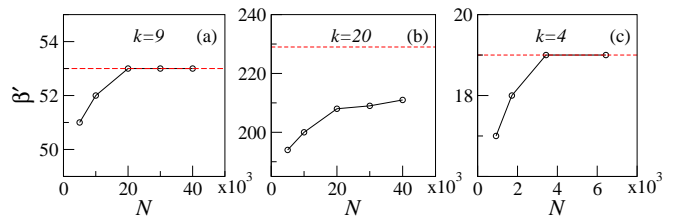


FIG. 5. Variation of β' as a function of matrix dimension N , for random matrices of the GOE class, for (a) $k = 9$ and (b) $k = 20$. For $k = 9$ it seen that β' converges to the predicted value ($k = 53$) as N increases, while for $k = 20$, a steady increase of β' towards the predicted value $k = 229$, is observed. (c) Variation of β' as a function of matrix dimension N for a GOE spin chain. For $k = 4$, as N increases, β' converges to 19, the predicted value.

based on Eq. 4, the expected value of $\beta' = 53$. Fig. 5(a) shows the convergence to this predicted value as the order N of the random matrix increases. In the other case, for $k = 20$ Eq. 4 predicts β' to be 229. However, as seen in Fig. 5(b), the convergence to the predicted value of β' is rather slow, and up to $N=40000$ for which spectra was computed it had not converged at all. Fig. 5(c) shows the same effect for the GOE spin chain for $k = 4$ as a function of size of Hilbert space for the system. In this case, the dimension N of the Hamiltonian matrix increases upon increasing the length L of the spin chain.

In physical systems, it is well-known that purely quantum effects such as tunneling and localization lead to deviations from random matrix averages. It may be noted that this effect comes into play for $k \gtrsim 5$ in some of the systems discussed in this work. Hence, in physical systems, the deviations could arise due to both physical effects that are not accounted for by RMT-type universality and also the finite size effects. By studying these deviations in physical systems from expectations based on Eqs. 3-4 and comparing it with random matrices of identical dimensions in which the deviations are purely due to finite size effects, it might be possible to distinguish whether the deviations occur due to finite size effects or system-dependent causes. The distribution of higher order ratios may then be useful to differentiate between and understand the effect of random and system-dependent fluctuations in a given physical system.

In summary, a generalized form of the Wigner surmise has been proposed to obtain a form for the distribution of *non-overlapping* spacing ratios of higher orders, in which the Dyson index $\beta \geq 4$ for the Gaussian and circular ensembles of random matrix theory. An elegant scaling relation is observed, relating the order k of the spacing ratio and the Dyson index β , to another constant β' . Effectively, for large random matrix sizes $N \gg 1$, the form of distribution of higher order spacing ratios $P^k(r, \beta')$ may be obtained for any arbitrary k , given the class of random matrices being considered. Eq. 4 also holds good for integer values of $\beta > 0$. For sufficiently small N and large k , finite size effects do tend to induce deviations

from the proposed scaling relation. It has been shown that convergence to scaling relation can be restored by increasing the dimension of the random matrix. In some cases, convergence to the predicted value was observed to be faster when the k -th order ratios considered were calculated in a completely non-overlapping manner, i.e. in Eq. 2, i increases in steps of k . Here, the numerator of the i^{th} ratio, would be the denominator of the $(i+1)^{\text{th}}$ ratio. The scaling relation Eq. 4 remains unchanged when the distribution of these ratios are considered as well.

These results have been shown to hold for several different physical systems, namely, spin chains belonging to GOE and GUE class, chaotic billiards, Floquet systems, all of whose eigenvalue fluctuations properties are well described by the Gaussian and circular ensembles of ran-

dom matrix theory. It must be noted that higher order spacing ratios are far easier to compute compared to the spacing distribution beyond the nearest neighbor. The results proposed here are of inherent interest in random matrix theory and provide large number of additional statistic to easily test the fluctuation properties of physical systems for putative RMT-type behavior. The rigorous numerical results proposed in this work should lead to attempts to obtain analytical justification for them.

Acknowledgements: The authors acknowledge Sanku Paul for providing data for the levels of the intermediate map. UTB acknowledges the funding received from Department of Science and Technology, India under the scheme Science and Engineering Research Board (SERB) National Post Doctoral Fellowship (NPDF) file number PDF/2015/00050.

* E-mail: harshini.t@gmail.com

† E-mail: udaybhosal0786@gmail.com

‡ E-mail: santh@iiserpune.ac.in

¹ H. Hasegawa, and Y. Sakamoto, Progress of Theoretical Physics Supplement, **139**, 112-127 (2000); S. M. Nishigaki, Physical Review E, **59**(3), 2853 (1999).

² S. D. Geraedts, R. Nandkishore and N. Regnault, Physical Review B, **93**(17), 174202 (2016).

³ L. Reichl, *The Transition to Chaos: Conservative Classical Systems and Quantum Manifestations*, Springer Science and Business Media (2013).

⁴ O. Bohigas, M. J. Giannoni and C. Schmidt, Phys. Rev. Lett. **52**, 1 (1984).

⁵ E.P. Wigner, Mathematical Proceedings of the Cambridge Philosophical Society, **47**(4), 790 (1951).

⁶ J.X. Zhong, U. Grimm, R.A. Roemer and M. Schreiber, Phys. Rev. Lett. **80**(18), 3996 (1998); F. Siringo, and G. Piccitto, Journal of Physics A: Mathematical and General, **31**(28), p.5981 (1998).

⁷ R. Modak, S. Mukerjee, and S. Ramaswamy, Physical Review B **90**(7), 075152 (2014); M. Serbyn and J.E. Moore, Phys. Rev. B, **93**(4), 041424 (2016).

⁸ H. J. Stöckmann, *Quantum Chaos: An Introduction*, Cambridge U.P. (2000).

⁹ K.M. Atkins and G.S. Ezra, Phys. Rev. E, **51**(3), 1822 (1995).

¹⁰ H. Friedrich and H. Wintgen, Phys. Rep. **183**(2), 37 (1989).

¹¹ H. A. Weidenmüller and G. E. Mitchell, Rev. Mod. Phys. **81**, 539 (2009); F. M. Izrailev, Physics Reports **196**(5-6), 299 (1990); H. J. Stöckmann and J. Stein, Phys. Rev. Lett. **64**(19), 2215 (1990); D. Delande, and J. C. Gay, Phys. Rev. Lett. **57**(16), 2006 (1986).

¹² M. Serbyn and J. E. Moore, Phys. Rev. B **93**, 041424(R) (2016); J. A. Kjäll, Phys. Rev. B **97**, 035163 (2018); E. Canovi, New J. Phys. **14**, 095020 (2012); R. Vosk, D. A. Huse and E. Altman, Phys. Rev. X **5**, 031032 (2015); V. K. Varma *et. al.*, J. Stat. Mech. 053101 (2017); P. Sierant, D. Delande and J. Zakrzewski, Phys. Rev. A **95**, 021601(R) (2017).

¹³ V. Oganesyan, D. A. Huse, Phys. Rev. B **75**, 155111 (2007).

¹⁴ C. Kollath, G. Roux, G. Biroli and A. M. Läuchli, J. Stat. Mech. P08011 (2010); M. Collura, H. Aufderheide, G. Roux and D. Karevski, Phys. Rev A **86**, 013615 (2012).

¹⁵ Y. Y. Atas, E. Bogomolny, O. Giraud, and G. Roux, Phys. Rev. Lett. **110**, 084101 (2013).

¹⁶ Y. Y. Atas *et. al.*, J. Phys. A : Math. Theor. **46**, 355204 (2013).

¹⁷ There is no unique definition of higher spacing ratio and here we adopt the convention that non-overlapping ratio implies no shared eigenvalue spacing between the numerator and denominator in Eq. 2. See Ref.¹⁶ for one result related to *overlapping* higher order spacing ratio distribution.

¹⁸ M. Brack and R. K. Bhaduri, *Semiclassical Physics*, Westview Press (2003); M.C. Gutzwiller, *Chaos in Classical and Quantum Physics*, Springer New York (1990).

¹⁹ K. Agarwal *et. al.*, Ann. Phys. **529**, 1600326 (2017).

²⁰ V. E. Kravtsov, I. M. Khaymovich, E. Cuevas, M. Amini, New J. Phys. **17**(12), 122002 (2015).

²¹ P. B. Kahn and C. E. Porter, Nucl. Phys. **48**, 385 (1963).

²² A. Y. Abul-Magd, and M. H. Simbel, Physical Review E, **60**(5), 5371 (1999).

²³ M.L. Mehta and F.J. Dyson, Journal of Mathematical Physics, **4**(5) (1963).

²⁴ D. C. Boes, F. A. Graybill and A. M. Mood, *Introduction to the theory of statistics, 3rd ed.*, New York: McGraw-Hill (1974).

²⁵ Aviva Gubin and Lea F. Santos, American Journal of Physics **80**(3), 246 (2012).

²⁶ H.I. Liou, H. S. Camarda, S. Wynchank, M. Slagowitz, G. Hacken, F. Rahn, and J. Rainwater, Physical Review C **5**(3), 974 (1972).

²⁷ Y. Avishai, J. Richert, and R. Berkovits, Phys. Rev. B **66**, 052416 (2002).

²⁸ Paul So, Steven M. Anlage, Edward Ott, and Robert N. Oerter, Phys. Rev. Lett. **74**, 2662 (1995).

²⁹ Fritz Haake, M. Kuś, and Rainer Scharf, Zeitschrift für Physik B Condensed Matter **65**(3), 381 (1987).

³⁰ Remy Dubertrand, Ignacio Garcia-Mata, Bertrand Geogot, Olivier Giraud, Gabriel Lemarie, and John Martin, Phys. Rev. E **92**, 032914 (2015).